Hydrophobic Properties of Phytochrome As Probed by 8-Anilinonaphthalene-1-sulfonate Fluorescence†

Tae-Ryong Hahn and Pill-Soon Song*

ABSTRACT: 8-Anilinonaphthalene-1-sulfonate (ANS) complexes with phytochrome, exhibiting a higher affinity for the Pfr form of phytochrome than for the Pr form. ANS fluorescence is enhanced by the additional binding of ANS to Pfr upon transformation of phytochrome from Pr to Pfr. The specific site of ANS binding appears to be the hydrophobic surface area of the protein, which becomes at least partially exposed in the Pfr form. An exposed, hydrophobic surface area in the Pfr phytochrome has been confirmed by the effects of ANS on the phototransformation of phytochrome. ANS accelerates the Pr → Pfr phototransformation, and it inhibits Pfr → Pr photoreversion and dark reversion. These effects are interpretable in terms of competitive binding of ANS to the chromophore binding site. Binding of ANS results in a drastic bleaching of the chromophore's absorption bands at 660 and 730 nm, particularly of the latter. This can be attributed to the exposed chromophore, which tends to resume a cyclic conformation with concomitant blue shift and hypochromism of the Q_y bands. Sodium dithionite counteracts the inhibitory effects of ANS on the dark reversion of Pfr to Pr, and its effect on the biphasic kinetics of the reversion has been discussed in terms of the Pfr model proposed.

Phytochrome acts as the red light photoreceptor for morphogenic responses in plants, and its phototransformation by red light from a physiologically inactive form, Pr, to the physiologically active form, Pfr, underlies the mechanism of photoreception (Hendricks et al., 1962; see recent reviews: Briggs & Rice, 1972; Pratt, 1978; Kendrick & Spruit, 1977; Rüdiger, 1980). Although the chemical structure of the Pr form is now well established, particularly with respect to the thioether linkage between the chromophore and protein (Klein & Rüdiger, 1978; Rüdiger, 1980; Lagarias & Rapoport, 1980), the mechanism of the phytochrome phototransformation and its role in triggering the initial event in morphogenic response processes largely remain obscure.

Elucidation of the mechanism of phototransformation of phytochrome and its role in morphogenic changes in plants may be approached at three different levels: (i) chemical mechanistic aspects of the chromophores of Pr and Pfr forms (Klein & Rüdiger, 1978; Lagarias & Rapoport, 1980; Song et al., 1979); (ii) characterization of the protein in the phototransformation [Song et al., 1979; Hunt & Pratt, 1981; Tobin & Briggs, 1973; Roux & Hillman, 1970; Mumford & Jenner, 1971; see Briggs & Rice (1972) for review]; and (iii) demonstration of the specific interactions of Pfr with its "receptor" and cellular organelles (Satter & Galston, 1976; Quail et al., 1973; Furuya, 1976). Understanding the photomorphogenic receptor from all these approaches still remains largely speculative.

In an attempt to characterize the phytochrome protein, we describe the use of a fluorescence probe (ANS) for elucidating hydrophobic properties of the Pr and Pfr forms of phytochrome. In our previous studies (Song et al., 1979; Song, 1980a), we proposed a working model for the phototransformation of Pr to Pfr by incorporating chemical transformation of the chromophore and resulting changes in apoprotein properties into the model. The model accommodates the following essential features: (a) Pr and Pfr chromophores have similar conformations; (b) the former is more rigidly held to the protein than is the latter, which is thus more exposed and flexible; and (c) as a consequence of the phototransformation of phytochrome accompanied by release of a SH group from the thioether linkage to the chromophore, the protein surface of Pfr, notably the chromophore contact area, is hydrophobic and available for interactions with an as yet unidentified Pfr hydrophobic receptor. Several lines of evidence in support of this model have been reviewed elsewhere (Song, 1980a). In this report, we discuss the hydrophobic properties of Pr and Pfr in terms of the ANS fluorescence probe.

8-Anilinonaphthalene-1-sulfonate (ANS) has been extensively used as a hydrophobic probe for proteins and membranes [see Brand & Gohlke (1972) for review]. Upon binding to hydrophobic sites of proteins or membranes, ANS emits intense blue fluorescence which is similar to that observed in nonpolar solvents. It emits only very weak green fluorescence in aqueous solution. In the present study, the effects of ANS binding to phytochrome on phytochrome absorption, phytochrome phototransformation, and dark reversion from Pfr to Pr, as well as effects on fluorescence properties, have been examined.

Materials and Methods

Materials. Undegraded phytochrome was isolated and purified from etiolated oat seedlings (*Avena sativa* L., CV Garry] as described proviously (Song et al., 1979). Usually, 4 kg of oat seedling tissues was extracted for brushite chromatography, followed successively by Sephadex G-25, DEAE-cellulose chromatography, and Sephadex G-200. In each final preparation, 15–20 mg of phytochrome with absorbance ratios (A_{280}/A_{660}) ranging from 1.6 to 2.7 were recovered from 60–70 mg of phytochrome present after the initial brushite chromatography. These phytochrome preparations were used for experiments which were not affected by purity index values, A_{280}/A_{660}. In independent experiments, the phytochrome prepared by the "conventional" procedure outlined above behaves identically as that ($A_{280}/A_{660} \lesssim 1.4$) prepared by immunoaffinity chromatography (Hunt & Pratt, 1979; Oh, 1980) and with "conventionally" prepared phytochrome with lower A_{280}/A_{660} ratios ($\sim$1.4).

An affinity chromatography was also used to prepare pure phytochrome, based on Affi-gel blue (Bio-Rad) chromatog-

† From the Department of Chemistry, Texas Tech University, Lubbock, Texas 79409. *Received October 13, 1980.* This work was supported in part by the Robert A. Welch Foundation (D-182) and the National Science Foundation (PCM79-06806).

0006-2960/81/0420-2602$01.25/0

raphy (Smith & Daniels, 1980). Phytochrome preparations (usually 20–25 mg) from brushite column were subjected to the Affi-gel chromatography. Phytochrome in the Affi-gel column was eluted with 10 mM FMN and then fractionally precipitated with ammonium sulfate. After the final step with Bio-Gel A 0.5 m column chromatography, 8–10 mg of phytochrome with a ratio of A_{280}/A_{660} equaling 1.38–1.76 was recovered. These phytochrome preparations were used for all fluorescence measurements (fluorescence spectra, polarizations, and lifetimes). We found no significant differences in spectral behaviors between conventional and Affi-gel phytochrome preparations. However, there are other subtle differences which will be reported elsewhere (Kim et al., 1981). Unless specified otherwise, all phytochrome solutions were in 0.1 M phosphate buffer, pH 7.8, containing 50 mM KCl and 1 mM EDTA.

All chemicals including ANS were reagent grades, purchased from Sigma Chemical Co., St. Louis, MO. ANS was recrystallized 3 times from dilute aqueous $MgCl_2$ before use (Penzer, 1972). Purified ANS gave a single spot when subjected to thin-layer chromatographic analysis (R_f 0.85 on alumina plate; solvent system, 1-butanol–ethanol–aqueous NH_3–water 200:47:3:88 v/v). Deionized water was glass redistilled for all buffers and solutions used in phytochrome purification and sample preparations.

Methods. All experiments were done at ice bath temperature (~273 K), under safe green light. Absorption spectral measurements for equilibrium and kinetic runs were performed on a Cary 118C spectrophotometer. Corrected emission and excitation spectra were recorded on a Perkin-Elmer Model MPF3 spectrofluorometer. Fluorescence polarizations were measured with an SLM Model 480 phase-modulation spectrofluorometer, utilizing sinusoidally modulated continuous light from a 1-kW Xe lamp. Fluorescence lifetimes were measured with the same instrument, obtaining both phase and modulation lifetimes at 10 and 30 MHz. Circular dichroic (CD) spectra were recorded on a JASCO-20 CD-ORD spectropolarimeter which was modified to enhance the signal-to-noise ratio by replacing the Pockels cell with a Morvue PEM-3 photoelastic modulator and with a lock-in amplifier (PAR 121) as described previously (Jung et al., 1980).

Irradiation of phytochrome for assay purposes based on the photostationary state of Pr and Pfr was carried out by using a simple accessory for the Cary 118C spectrophotometer (Jung & Song, 1979). Irradiation of phytochrome for its phototransformation experiments was carried out with a Bausch & Lomb microscopic illuminator combined with a 660-nm interference filter for the red light source to ensure the monochromaticity of irradiation and with an infrared cutoff filter for the far-red light source. Fluence rates used were 7.5 W/m^2 and 1.6 kW/m^2 for red and far-red light irradiations, respectively. All irradiations were performed in a cold chamber or ice bath to prevent any heating effect of actinic light and degradation of phytochrome during experiments.

Results

Figure 1 shows the absorption spectra of Pr and Pfr in the presence and absence of ANS. It can be readily seen that the absorption spectra of both Pr and Pfr are profoundly affected by millimolar or less concentrations of ANS. The Q_y band (660 nm) of Pr exhibits hypochromicity upon addition of ANS (Figure 1A). With increasing ANS concentrations, absorbance at the red edge ($\lambda > 700$ nm) increases slightly, and an isosbestic point occurs at ca. 700 nm, along with an increase in absorbance at $\lambda < 600$ nm. An apparent blue shift of the λ_{max} of Pr to 658 nm (spectrum 6) occurs due to the complexation of Pr with ANS and partly due to an increased absorption of ANS which underlies the wavelength region 500–600 nm (vide infra).

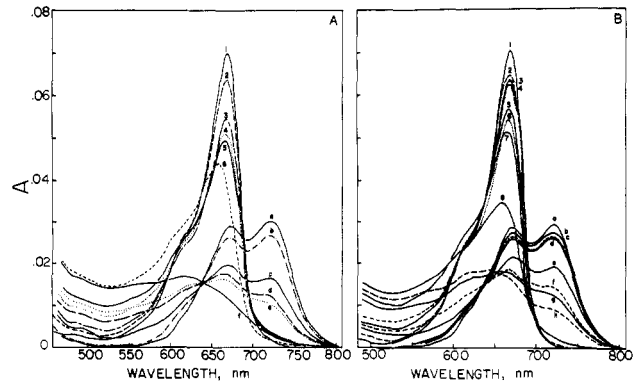

FIGURE 1: Effects of ANS on the absorption spectra of phytochrome in phosphate buffer, pH 7.8, 273 K. (A) The absorption spectra of Pr were recorded after mixing it with specified concentrations of ANS, while those of Pfr were obtained by red-light irradiation of the mixtures Pr + ANS. Spectra 1–6: [Pr] = 1 μM, [ANS] = 0.00, 0.20, 0.50, 1.00, 1.50, and 2.00 mM, respectively. Spectra a–f: [Pfr] = 0.8 μM, [ANS] = 0.00, 0.20, 0.50, 1.00, 1.50, and 2.00 mM, respectively. (B) The absorption spectra of Pfr were obtained by first photoproducing Pfr from Pr in the absence of ANS, followed by the addition of specified ANS concentration. The absorption spectra of Pr were obtained by far-red irradiation of Pr + ANS mixtures. Spectra a–h: Pfr = 0.8 μM, [ANS] = 0.00, 0.05, 0.10, 0.20, 0.50, 1.00, 1.50, and 2.00 mM, respectively. Spectra 1–8: Pr = 1 μM, [ANS] = 0.00, 0.05, 0.10, 0.20, 0.50, 1.00, 1.50, and 2.00 mM, respectively.

The effect of ANS on Pfr is even more drastic than that on Pr (Figure 1A). Increases in ANS concentrations induce strong hypochromism of the Q_y band (725 nm) of Pfr as well as a blue shift to 620 nm (spectrum f). An isosbestic point occurs at 640 nm. At the concentrations of ANS used, no evidence for the denaturation of protein was apparent, as monitored by CD in the UV region. ANS added to Pfr after the latter was photoproduced from Pr exerts similar effects on the absorption spectra of Pfr and Pr; the Pr here was produced by far-red irradiation of Pfr after ANS was added (Figure 1B). However, at higher concentrations of ANS, recovery of Pr from Pfr was retarded (compare spectrum 8 in Figure 1B with spectrum 6 in Figure 1A). Some difference can also be seen between spectrum h in Figure 1B and spectrum f in Figure 1A, again suggesting that interactions between ANS and phytochrome show hysteresis, particularly at ANS concentrations higher than 1 mM (Figure 1). The absorbance ratio of Pr (A_{660}^{Pr}) to Pfr (A_{725}^{Pfr} and A_{660}^{Pfr}) substantially increased with increasing ANS concentrations (Figure 1). As noted above, Pfr is almost completely bleached in the 730-nm region at 2 mM ANS (Figure 1).

Figure 2 shows the fluorescence emission spectra of ANS, which becomes strongly fluorescent upon complexation with Pr and Pfr. Table I summarizes the ANS fluorescence data. From both Figure 2 and Table I, it can be seen that the ANS fluorescence emission is significantly enhanced upon Pr to Pfr phototransformation of the phytochrome–ANS mixture. This enhancement is reproducible and can be attributed to the additional binding of ANS to Pfr. The enhanced binding of ANS to Pfr over Pr can also be confirmed by the fluorescence polarization data shown in Table II. As free ANS binds to protein and becomes fluorescent, its fluorescence polarization is expected to increase. Thus, an additional binding of ANS to Pfr is demonstrated by the increase in fluorescence polarization upon Pr → Pfr transformation (Table II). Fluorescence lifetimes of ANS also increase upon Pr → Pfr transformation, parallel with the increasing values for fluorescence

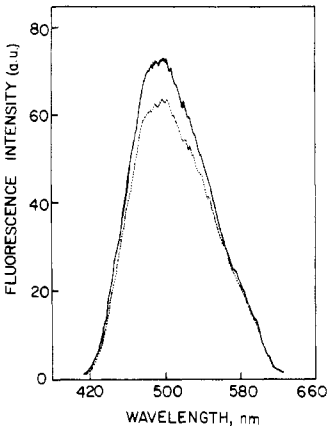

FIGURE 2: Fluorescence enhancement of ANS (1 mM; solid line) upon transformation of Pr (dotted line) (1.0 μM) to Pfr (0.8 μM at photostationary equilibrium), in 0.1 M phosphate buffer, pH 7.8, 273 K. Excitation wavelength, 410 nm; bandpass for excitation, 6.4 nm; bandpass for emission, 3 nm.

Table I: Effect of the Pr → Pfr Phototransformation on the Fluorescence of Bound ANS[a]

phytochrome (μM)	ANS (μM)	fluorescence enhancement[b] (%)
1.6	0	0[c]
1.6	390	5.1[c]
1.0	500	6.2[c]
1.0	1000	9.6[c]
0.053	0.5	0[d]
0.352	0.5	3[d]
0.528	0.5	14[d]
0.880	0.5	31[d]

[a] Conditions as described in the caption to Figure 2. [b] Defined as $\Delta I_F^{Pr\rightarrow Pfr} \times 100/I_F^{Pr}$, where I_F^{Pr} and $\Delta I_F^{Pr\rightarrow Pfr}$ represent ANS fluorescence intensities before and after Pr → Pfr phototransformation; $\Delta I_F^{Pr\rightarrow Pfr}$ was measured immediately upon Pfr formation from Pr incubated for 2–5 h in the presence of ANS. Average of ten measurements. [c] Using Pr from "Affi-gel" procedure with highest purity (virtually free of contaminant proteins). [d] Using Pr obtained from "conventional" procedure and values corrected for ANS fluorescence attributable to contaminant proteins.

Table II: Fluorescence Polarization of ANS Bound to Phytochrome in Phosphate Buffer, pH 7.8, 273 K

[Pr] (μM)	[ANS] (μM)	λ_{ex} (nm)	polarization (P) Pr	Pfr	ΔP[a]
1.0	500	400	0.244 ± 0.008	0.254 ± 0.014	0.010
		420	0.267 ± 0.008	0.273 ± 0.007	0.007
		430	0.297 ± 0.009	0.305 ± 0.014	0.008
1.6	60	390	0.311 ± 0.014	0.321 ± 0.013	0.010
	390	380	0.231 ± 0.009	0.246 ± 0.009	0.015
		390	0.253 ± 0.007	0.267 ± 0.008	0.014
		400	0.274 ± 0.009	0.288 ± 0.011	0.014
		410	0.280 ± 0.007	0.306 ± 0.002	0.026
		420	0.294 ± 0.010	0.304 ± 0.009	0.010
		430	0.327 ± 0.014	0.338 ± 0.011	0.011
		440	0.290 ± 0.023	0.306 ± 0.022	0.016

[a] $\Delta P = P(Pfr) - P(Pr)$.

intensity and polarization (Table III). From the variations in lifetime as a function of modulation mode and frequency for the lifetime measurements (Table III), it can be seen that the decay of ANS fluorescence emission is not exponential.

In order to elucidate the nature of hypochromism (bleaching of the Q_y band) by ANS (Figure 1), we also examined the CD spectra of phytochrome in the presence of ANS (Figure 3). Parallel with changes in the absorption spectra (Figure 1), the

Table III: Fluorescence Lifetimes (τ_F) of ANS Bound to Phytochrome (2.0 μM) in Phosphate Buffer, pH 7.8, 1 mM EDTA, 50 mM KCl, 273 K[a]

modulation frequency (MHz)	mode	τ_F (ns) Pr-ANS	Pfr-ANS
30	modulation (m)	9.75 ± 0.07	10.27 ± 0.09
	phase shift (ϕ)	5.59 ± 0.13	5.83 ± 0.13
10	m	21.43 ± 1.58	23.00 ± 0.26
	ϕ	8.99 ± 0.32	8.87 ± 0.43

[a] $[ANS]_{total}$ = 500 μM; λ_{ex} 395 nm; λ_{em} 480 nm.

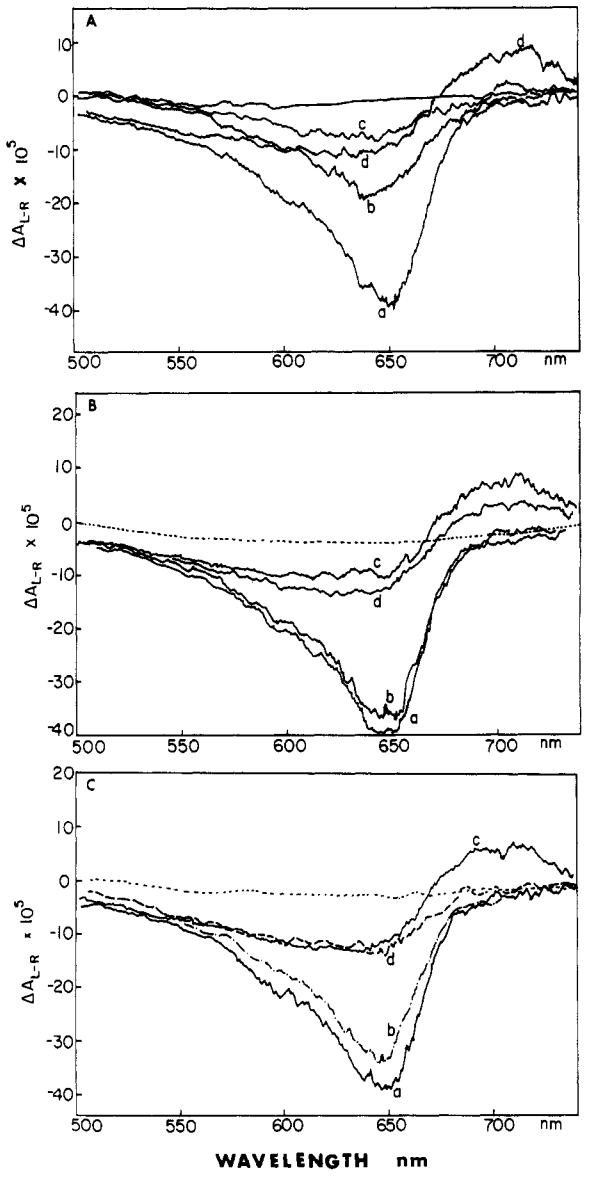

FIGURE 3: CD spectra of Pr and Pfr (~80% photostationary concentration, $[Pfr]_{eq}$, obtained from Pr with red light) in phosphate buffer (pH 7.8, 273 K) as a function of ANS concentration. ANS was added to Pfr after its phototransformation from Pr. (A) (a) [Pr] = 1.86 μM, [ANS] = 0 mM; (b) [Pr] = 1.60 μM, [ANS] = 2.07 mM; (c) $[Pfr]_{eq} \simeq$ 1.30 μM, [ANS] = 2.07 mM; (d) $[Pfr]_{eq} \simeq$ 1.50 μM, [ANS] = 0 mM. (B) (a) [Pr] = 1.86 μM, [ANS] = 20 μM; (b) [Pr] = 1.80 μM, [ANS] = 390 μM; (c) $[Pfr]_{eq} \simeq$ 1.50 μM, [ANS] = 20 μM; (d) $[Pfr]_{eq} \simeq$ 1.40 μM, [ANS] = 390 μM. (C) (a) [Pr] = 1.86 μM, [ANS] = 40 μM; (b) [Pr] = 1.72 μM, [ANS] = 1.111 mM; (c) $[Pfr]_{eq} \simeq$ 1.50 μM, [ANS] = 40 μM; (d) $[Pfr]_{eq} \simeq$ 1.40 μM, [ANS] = 1.111 mM.

negative CD signal for Pr is gradually bleached and blue shifted with increasing ANS concentrations. The bleaching rate is much faster for the positive signal of Pfr than the

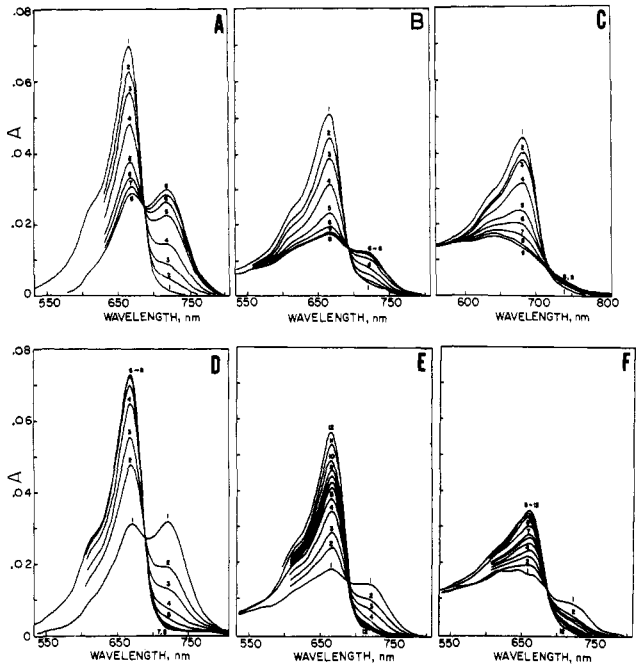

FIGURE 4: (Top) Changes in the absorption spectra of phytochrome (Pr; 1 μM) in phosphate buffer, pH 7.8, 273 K, as a function of irradiation with 660-nm light (fluence rate ~7.5 W/m^2) in the presence of ANS (for panels A, B, and C). (A) [ANS] = 0 mM; spectra 1–8 at 0.0 (no irradiation), 1.8, 3.6, 7.2, 14.4, 21.6, 32.4 and 92.4 s, respectively, upon irradiation. (B) [ANS] = 1.0 mM; spectra 1–8 have the same time scale as in (A). (C) [ANS] = 2.0 mM; spectra 1–8 have the same time scale as in (A). (Bottom) Changes in the absorption spectra of phytochrome ($[Pfr]_{eq}$ produced from 1 μM Pr, in the absence of ANS), in phosphate buffer, pH 7.8, 273 K, as a function of irradiation with 730-nm light (fluence rate 1.6 kW/m^2) in the presence of ANS. ANS was added to Pfr after it was photoproduced from Pr (D–F). (D) [ANS] = 0 mM; spectra 1–8 have the same time scale as in (A). (E) [ANS] = 1.0 mM; spectra 1–8 have the same time scale as in (A). Spectra 9–12: 210, 330, 690, and 1410 s, respectively, upon irradiation. (F) [ANS] = 2.0 mM; spectra 1–8 have the same time scale as in (A). Spectra 9–12: same time scale as in (E).

negative CD signal of Pr. Although CD signals below 500 nm were not accurately measurable due to a voltage saturation of the detector PMT arising from high absorbances by ANS, it was apparent that no significant changes were observed in the UV region. However, the CD band at 370–390 nm of Pr and Pfr was substantially bleached by the added ANS.

To elucidate the spectral perturbation of phytochrome by ANS shown in Figures 1 and 3, we have looked at spectral changes of Pr and Pfr as a function of their phototransformation and ANS concentrations. Results are shown in Figure 4 (isosbestic point at 689 nm). As the ANS concentration increases, appearance of the far-red absorption band of Pfr upon red-light irradiation of Pr diminishes (Figure 4B), and eventually the far-red absorption disappears, even though the "reversible" photobleaching at 660 nm still persists (Figure 4C). Thus, these results are indicative of dark bleaching of Pfr by complexation with ANS as soon as it is photoproduced from Pr. This spectral behavior is consistent with spectral changes of Pfr upon addition of ANS and phototransformation to Pr (Figure 4D–F). Again, with increasing ANS concentrations, the 730-nm band is quickly bleached even before far-red light was applied (e.g., compare the absorbances at 730 nm for spectra 1 in Figure 4D,E). Furthermore, far-red irradiation at 730 nm, where absorbance is less than 0.01, still produces Pr (see Figure 4E,F). In other words, Pr seems to be produced from its precursor, which does not significantly absorb the 730-nm actinic light. One plausible explanation

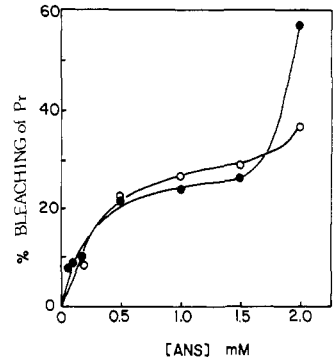

FIGURE 5: Bleaching of phytochrome (Pr, 1.0 μM) in phosphate buffer, pH 7.8, 273 K, as a function of ANS concentration. (○) Bleaching of Pr by ANS prior to its phototransformation of Pfr. (●) Bleaching of Pr after its photoproduction from Pfr, in the presence of ANS. Per cent bleaching is defined as $(A_{660}^{ANS} \times 100)/A_{660}^{0}$, where A_{660}^{ANS} and A_{660}^{0} are absorbances with and without added ANS, respectively.

is that Pr is produced from trace amounts of free Pfr, which is at dynamic equilibrium with its ANS complex.

From Figure 1, data on the bleaching of Pr by ANS, prior to its phototransformation to Pfr and regeneration (or cycling) by photoreversion from the Pfr form can also be obtained (see Figure 5). Bleaching of Pr is approximately the same at ANS concentrations below 1.5 mM regardless of whether or not Pr was cycled. However, at 2 mM ANS, the Pr which has experienced one cycling (i.e., prepared from Pfr in the presence of ANS) shows more extensive bleaching than does the Pr without cycling. This means that the binding of ANS to Pr and Pfr exhibits hysteresis because of preferential binding of ANS to the latter (vide supra).

To ascertain whether or not intermediate(s) produced during the phototransformation of phytochrome (Pr → Pfr and Pfr → Pr) are trapped by ANS, we examined the effect of phytochrome photocycling on ANS-induced spectral perturbation as a function of irradiation. Figure 6 shows the results. A close comparison of the spectra of Figure 6A with those in Figure 4 yields no significant differences at ~1 mM ANS. However, at higher concentrations (e.g., 2 mM), the bleaching of both Pr and Pfr is more pronounced with the photocycled Pr (Figure 6B) than with the uncycled Pr (Figure 4C). This suggests that some intermediates, along with Pr and Pfr, are indeed "trapped" by ANS. Similarly, the photocycled Pfr is more strongly bleached by ANS (Figure 6C,D) than the uncycled Pfr (Figure 4F), bleaching being more pronounced at the far-red absorption band than at the red absorption band (Figure 6).

Figure 7 presents the effects of ANS on the phototransformation of phytochrome. In all samples, the Pr → Pfr phototransformation is nearly completed within 30 s of red-light application. However, the disappearance of Pr absorption at 660 nm is not quantitatively matched with the appearance of the far-red absorption by Pfr, as the ANS concentration increases (Figure 7A). The photoreversion from Pfr to Pr exhibits apparent anomalies. With low concentrations (below 200 μM), the photoreversion is nearly complete within 20 s of far-red application (Figure 7B). At 0.5–2.0 mM ANS, however, completion of the photoreversion is extremely slow, in spite of the fact that the absorbance change at 730 nm has leveled off quickly, well within 30 s of irradiation (Figure 7B).

Pr → Pfr phototransformation apparently follows first-order kinetics, as the rate of disappearance of Pr is determined by the intensity of light absorbed (Figure 8A). While Pr → Pfr phototransformation follows first-order kinetics with or without added ANS, the effect of the latter on their transformation rates is peculiarly dual. An increase in ANS concentration

Table IV: Rate Constants Obtained from Linear Regression Analyses of the Kinetics of the Phototransformations of Phytochrome (1 μM) in Phosphate Buffer (pH 7.8) at 273 K with 660 nm (7.5 W/m^2) and 730 nm (1.6 kW/m^2) Light, as a Function of ANS Concentration[a]

	Pr → Pfr		Pfr → Pr		
[ANS] (μM)	k_0 (s^{-1})	relative k_0	k_1 (s^{-1})	k_2 ($s^{-1} \times 10^2$)	k_2 component[b] (%)
0	0.098	1.0	0.24	0	0
50			0.22	0	0
100			0.22	0	0
200	0.114	1.17	0.27	7.52	22
500	0.123	1.26	0.28	2.23	28
1000	0.131	1.34	0.27	1.97	57
1500	0.095	0.97	0.26	0.97	63
2000	0.072	0.73	0.28	0.98	66

[a] Correlation coefficient for the rate constants listed ranged from 0.997 to 1.00. [b] k_1 and k_2 for faster and slower components, respectively, and amplitude of the latter as resolved by the peeling procedure (Van Liew, 1967).

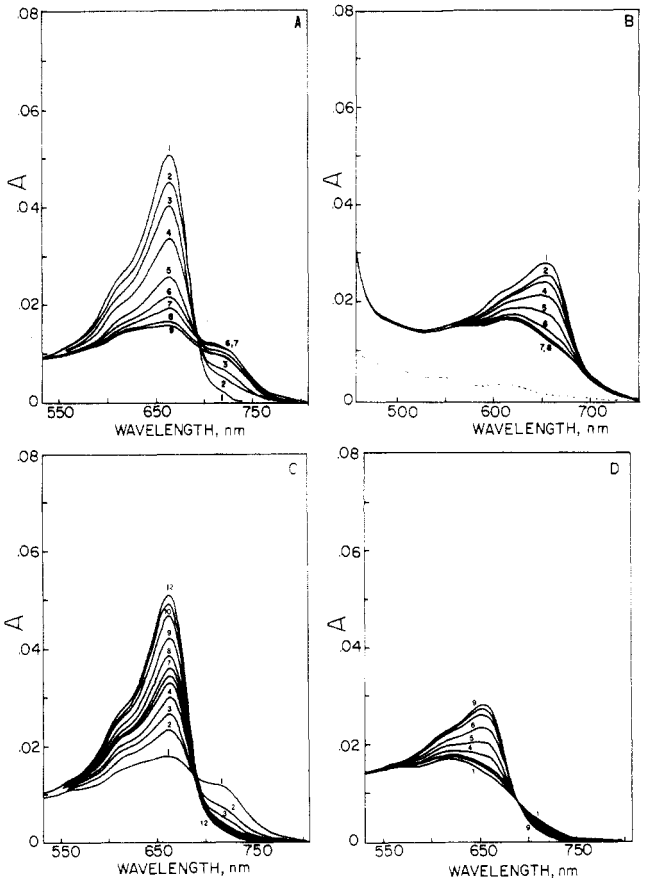

FIGURE 6: Effects of ANS on the absorption spectra of photocycled Pr

$$Pr \xrightarrow[ANS]{660\ nm} Pfr \xrightarrow[ANS]{730\ nm} Pr$$

and its phototransformation to Pfr with 660 nm light (7.5 W/m^2). (A) Pr was produced in the presence of [ANS] = 1.5 mM after 1 photocycle

$$Pr \xrightarrow[ANS]{660\ nm} Pfr \xrightarrow[ANS]{730\ nm} Pr$$

in phosphate buffer, pH 7.8, 273 K. [Pr] = 1.0 μM (unphotocycled original Pr). Spectra 1–9: 0.0, 1.8, 3.6, 7.2, 14.4, 21.6, 32.4, 92.4, and 210 s, respectively, after irradiation. (B) [ANS] = 2.0 mM; otherwise same as in (A). Spectra 1–8 have the same time scale as in (A). (C) Effects of ANS on the absorption spectra of photocycled Pfr

$$Pr \xrightarrow[ANS]{660\ nm} Pfr$$

and its phototransformation to Pr with 730-nm light (1.6 kW/m^2). $[Pr]_{initial}$ = 1.0 μM. Pfr was produced in the presence of [ANS] = 1.5 mM, in phosphate buffer, pH 7.8, 273 K. Spectra 1–9 have the same time scale as in (A). Spectra 10–12: 330, 690, and 1410 s, respectively. (D) Pfr was produced in the presence of [ANS] = 2.0 mM, in phosphate buffer, pH 7.8, 273 K. Otherwise same as in (C). Spectra 1–9 have the same time scale as in (C).

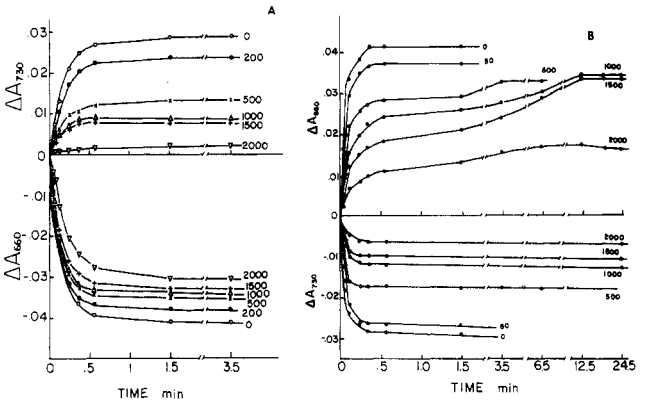

FIGURE 7: Phototransformation of phytochrome (phosphate buffer, pH 7.8, 273 K) as measured by the absorbance changes (ΔA_{660}, ΔA_{730}) at 660 and 730 nm upon irradiation of phytochrome–ANS mixtures (molar ratio of ANS to phytochrome is shown for each curve). (A) Pr (1.0 μM), 660 nm (7.5 W/m^2) for Pr → Pfr phototransformation. (B) Pfr (0.8 μM), 730 nm (1.6 kW/m^2) for Pfr → Pr phototransformation.

up to a molar ratio [ANS]/[Pr] of 1000 accelerates the rate, but concentrations higher than a 1500 molar ratio inhibit the phototransformation rate (Figure 8A). In photoreversion, these dual effects of ANS are absent; increasing ANS concentrations proportionately inhibits the reversion. However, while Pr → Pfr phototransformation apparently follows first-order kinetics with or without added ANS (Figure 8A), the photoreversion kinetics deviate from first order as ANS concentrations increase (Figure 8B). In fact, the rates of photoreversion in the presence of ANS at molar ratios [ANS]/[Pr] greater than 100 can be resolved into two components. Using the peeling procedure[1] (Van Liew, 1967), extrapolation of the slower component line (e.g., the curve at molar ratio 500 in Figure 8B) to the ordinate and subtraction of the extrapolated line from the observed curve result in a straight line if a faster kinetic component is present. Apparently, this is what happens in photoreversion curves with increasing ANS concentrations (Figure 8B). Apparent rate constants evaluated from these treatments are presented in Table IV. It can be seen that rate constants for the faster components remain essentially invariant with increasing ANS concentrations while the slower components decrease in rate but increase in relative amplitude as a function of ANS concentration.

In contrast to the enhancement of the Pr → Pfr phototransformation by ANS (Figure 8A) but parallel to the inhibition of photoreversion by ANS (Figure 8B), dark reversion is slowed down by ANS (Figure 8C). It is well-known that dark reversion shows biphasic kinetics (Correll et al., 1968;

[1] This procedure was previously applied to phytochrome reversion (Correll et al., 1968; Negbi et al., 1975).

Table V: Rate Constants Obtained from Linear Regression Analyses of the Kinetics of Dark Reversion (Pfr → Pr) of Phytochrome in Phosphate Buffer, pH 7.8, at 273 K, in the Presence of ANS and Sodium Dithionite[a]

[phytochrome] (μM)	[ANS] (mM)	[dithionite] (mM)	k_1 ($s^{-1} \times 10^4$)	k_2 ($s^{-1} \times 10^6$)	k_2 component[b] (%)	k_1/k_2[b]	$\%k_1/\%k_2$	dithionite acceleration[c] k_1^{rel}	dithionite acceleration[c] k_2^{rel}	rel (% $k_1/\%k_2$)[d]
2.4	0	0	7.23	7.71	75.0	93.8	0.33			
2.1	0.625	0	7.69	7.60	80.1	101.2	0.25			
2.1	1.25	0	7.70	4.92	91.2	156.5	0.10			
2.0	0	2.14	7.97	158.00	33.0	5.0	2.03	1.10	20.5	6.2
1.8	0.536	2.14	7.45	145.00	35.0	5.1	1.86	0.97	19.1	7.4
1.8	1.07	2.14	7.24	96.00	48.5	7.5	1.06	0.94	19.5	10.6

[a] Correlation coefficients for the rate constants listed ranged from 0.981 to 1.00. [b] Resolved by the Peeling procedure (Van Liew, 1967). [c] k_1^{rel} and k_2^{rel}, relative to $k_1 = 7.23 \times 10^{-4}$ s^{-1}, $k_2 = 7.71 \times 10^{-6}$ s^{-1} (first row). [d] Calculated relative to ($\%k_1/\%k_2$) as follows: 2.03/0.33 = 6.2, 1.86/0.25 = 7.4, and 1.06/0.10 = 10.6, respectively.

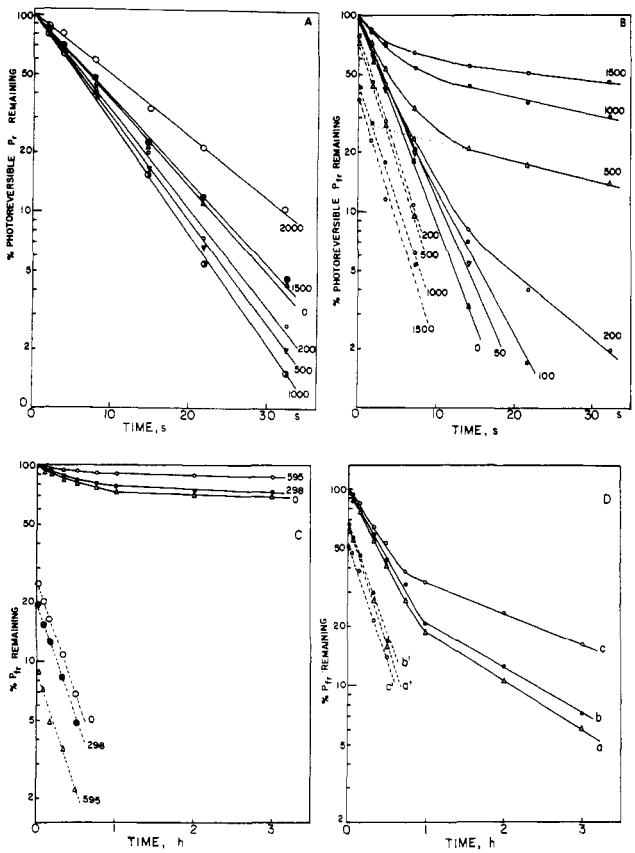

FIGURE 8: Kinetics of (A) Pr → Pfr phototransformation and (B) Pfr → Pr photoreversion, in phosphate buffer, pH 7.8, 273 K, as a function of ANS concentration (ratio [ANS]/[Pr] for each kinetic plot is shown). Fluence rate used: (A) 7.5 W/m^2 (660 nm); (B) 1.6 kW/m^2 (730 nm). Dotted lines in (B) represent the kinetics of faster decaying components calculated by the Peeling procedure of extrapolation–subtraction (e.g., see kinetic curve at [ANS]/[Pr] = 500 in (B)) as described in the text. Effects of (C) ANS and (D) ANS plus dithionite on the dark reversion of Pfr ($[Pfr]_{eq} \sim 1.5$ μM produced from [Pr] = 2.1 μM) in phosphate buffer, pH 7.8, 273 K. The molar ratios of ANS to phytochrome are shown (upper sets of curves). The faster kinetic components of respective reversion curves are shown in broken straight lines, as resolved by the extrapolation–subtraction procedure described in the text. (C) Dark reversion in the presence of ANS; molar ratios are indicated. [dithionite] = 0 mM. (D) Combined effects of ANS and sodium dithionite (2.14 mM). (a) Pfr + 0 mM ANS + dithionite: [ANS]/[Pfr] = 0, [dithionite]/[Pfr] = 1427. (b) Pfr + 0.54 mM ANS + dithionite: [ANS]/[Pfr] = 360, [dithionite]/[Pfr] = 1427. (c) Pfr + 1.25 mM ANS + dithionite: [ANS]/[Pfr] = 833, [dithionite]/[Pfr] = 1427. (a′–c′): faster kinetic components corresponding to (a–c); see text.

Pike & Briggs, 1972; Negbi et al., 1975). The faster components can be resolved by the peeling method (Figure 8C), and as can be seen they are not significantly affected by ANS. Dithionite is known to accelerate dark reversion (Pike & Briggs, 1972; Mumford & Jenner, 1971). We have confirmed

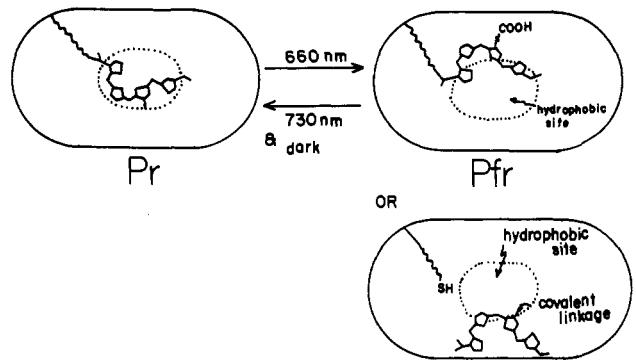

FIGURE 9: Simplified model for the phototransformation of Pr → Pfr (the reaction mechanism for the chromophores is not shown). Two models (shown) are possible for Pfr, depending on whether the propionic acid side chain in Pr is free (Lagarias & Rapoport, 1980) or the side chain is covalently linked in Pr and Pfr and a SH group is released (Song et al., 1979; Song, 1980a). The propionic acid side chain in phycobilins is covalently linked (Killilea et al., 1980).

this observation (see curve a, Figure 8D). However, the faster components, which are ANS-independent (Figure 8C), are unaffected by dithionite (Figure 8D and Table V).

Discussion

Our specific aim in this study was to probe the hydrophobic properties of phytochrome, particularly the Pfr form. It has been suggested that the major molecular event of biological significance in the phototransformation of physiologically inactive Pr to the active Pfr form of the photomorphogenic receptor is the development of a hydrophobic surface on the latter, without significant conformational changes in its chromophore and apoprotein[2] (Song et al., 1979; Song, 1980a). The proposed model is depicted in Figure 9, which facilitates the interpretation of results obtained with ANS as a fluorescence probe of the hydrophobic properties of phytochrome.

ANS exerts profound effects on the absorption spectra of phytochrome, particularly Pfr (Figure 1). Due to limited solubility of phytochrome, especially the Pfr form, Scatchard plots for the absorbance changes due to complex formation between phytochrome and ANS did not yield satisfactory binding isotherms (plots not shown). Double-reciprocal plots (Benesi–Hildebrand) of absorbance changes vs. ANS concentrations showed first positive then negative deviations. However, from the linear portions of the plots in the concentration range 0.2–2 mM ANS, apparent binding constants of 1×10^{-3} M (correlation coefficient 0.986) and 9×10^{-4} M

[2] We recently showed that the rotational relaxation times of Pr and Pfr are essentially identical, as determined by the fluorescence anisotropy of pyrene-*N*-maleimide and fluorescamine-labeled phytochromes, suggesting that no gross conformational changes of apoprotein occurs in the Pr → Pfr transformation (Song, 1980b; Oh, 1980).

(correlation coefficient 0.996) were obtained for Pr-ANS and Pfr-ANS complexes, respectively. From nonlinearity of these data, it is clear that more than one ANS is bound per protein. In the lower range of ANS concentrations, where the double-reciprocal plot showed a downward deviation, the apparent binding constants were estimated to be on the order of (2–6) $\times 10^{-5}$ M, suggesting that one phytochrome molecule binds two or more ANS molecules. This is clearly indicated by the nonexponential fluoresence lifetimes of ANS bound to the phytochrome (Table III). In a system of heterogeneous fluroescence decays, lifetime values obtained with a 30-MHz sinusoidal exciting beam should be shorter than those obtained with a 10-MHz beam; this is borne out in the data shown in Table III. Within the 30-MHz modulation frequency measurements, the lifetime from phase shift is expected to be shorter than that from modulation value (Spencer & Weber, 1969; Spencer, 1970; Lakowicz et al., 1980). This is also borne out in the present data (Table III). These long fluorescence lifetimes can be attributed to ANS tightly bound to the hydrophobic surface of Pr and Pfr. The dual catalytic and inhibitory effects of ANS on the phototransformation of Pr to Pfr (Figure 8) also suggest binding of more than one ANS per Pr.

As noted earlier, bleaching of Pfr at 730 nm exhibits hysteresis at concentrations of ANS greater than 1 mM. This suggests that intermediates and/or Pfr with different surface properties produced during the phototransformation (cycling) are selectively complexed with ANS, resulting in hysteresis in the bleaching curves (Figure 5). This is further confirmed by the fact that the apparent binding constant depends on the cycling of phytochrome.

Strong bleaching, blue shift, and loss of the CD signal (Figure 3) in the 730-nm band of Pfr are all consistent with the idea that the Pfr surface is more hydrophobic than the Pr surface (Song et al., 1979; Song, 1980a), as illustrated in Figure 9. Thus, ANS fluorescence enhancement by Pr → Pfr phototransformation (Figure 2, Tables I–III) lends further support for the model.

The molecular topography emerging from these observations is that, in the Pfr form, the hydrophobic chromophore binding site is already occupied by ANS, resulting in increased fluorescence parameters, while the chromophore forced out of the binding site assumes its stable, "circular" conformation (Song et al., 1979), resulting in the bleaching and blue shift of the 730-nm band. Thus, the spectral perturbations caused by ANS show somewhat similar changes caused by the denaturation of phytochrome, which exposes the chromophore (Butler et al., 1964). It should be noted that a free phytochrome chormophore assumes a "circular" conformation in the absence of a apoprotein (Song et al., 1979), with concomitant absorbance decrease and blue shift of the Q_y band (Song, 1978). The suggestion that the Pfr chromophore is more flexible and exposed than the Pr chromophore is further supported by our recent finding that the permanganate oxidation of the former proceeds much faster than does that of the latter (Hahn et al., 1980).

The preferential bleaching of Pfr as the result of ANS binding is further demonstrated by the data shown in Figure 4. As soon as Pfr is produced from Pr, it is effectively bleached by excess ANS. It is interesting to note that the Pfr → Pr photoreversion continues to occur even though very little actinic light at 730 nm is absorbed by the bleached Pfr (Figures 4 and 7). This can be explained by the dynamic equilibrium

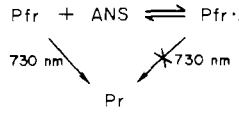

Scheme I

(i) In the absence of ANS

(ii) In the presence of ANS

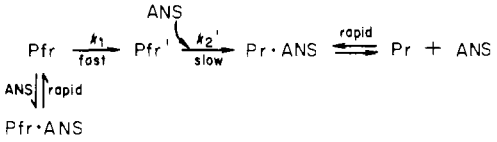

where the Pfr·ANS complex absorbs little at 730 nm as a result of the blue shift of the Q_y absorption maximum (Figures 1 and 4). The 1:1 stoichiometry of ANS binding shown is not meant to imply that only the 1:1 stoichiometry is involved.

It is noteworthy that ANS affects only the slower kinetic component in the photoreversion of Pfr, while the rate of the overall reversion is inhibited by ANS without decreasing the rate of the faster kinetic component (Figure 8). On the other hand, the Pr → Pfr phototransformation follows first-order kinetics; at low ANS concentrations the rate is accelerated, while the phototransformation is inhibited at higher concentrations (Table IV and Figure 8). The result suggests that ANS at lower concentrations acts as an activator in the Pr → Pfr transformation by facilitating loosening of the bound chromophore from its hydrophobic binding site. In the reversion, this chromophore binding site is now occupied by ANS, which thus acts as a competitive inhibitor for the photoreversion.

As in the photoreversion of Pfr, the dark reversion is also kinetically biphasic (Figure 8 and Table V). Again, the faster kinetic component is essentially unaffected by ANS, while the slower component is progessively inhibited by ANS. Others have reported the biphasic kinetics of the dark reversion of Pfr (Correll et al., 1968; Pike & Briggs, 1972; Negbi et al., 1975).

There are two alternative models to explain the biphasic kinetics of the Pfr dark reversion. The most widely assumed model is based on the existence of two sets of phytochrome populations (Taylor, 1968; Manabe & Furuya, 1971; Pike & Briggs, 1972; Negbi et al., 1975). The alternative model is based on a consecutive kinetic sequence involving two interacting chromophores (Pike & Briggs, 1972).

Results of the ANS experiments shown in Figure 8 and Tables IV and V are more consistent with a consecutive kinetic model but not necessarily with the two-chromophores model (it is generally agreed that there is only one chromophore per protein, although phytochrome may associate as dimers in solution: Pratt, 1978). It is difficult to explain the ANS effect since ANS will complex with both populations of Pfr if the two-population model were correct. We propose a simplified scheme to account for the biphasic kinetics and the effect of ANS on the dark reversion of Pfr (Scheme I). In this scheme, binding of ANS at nonspecific site(s) on the Pfr is not shown. Intermediate Pfr′ still absorbs at 730 nm, but its molar extinction coefficient is lower than that of Pfr·ANS complexes with Pfr′, thus retarding its rate (k_2') on conversion to Pr. Pfr·ANS and Pr·ANS complexes lose their strong Q_y absorbances, as discussed earlier.

Additional support for Scheme I comes from the data shown in Figure 8 and Table V. Dithionite and other reducing agents with diverse structure accelerate the dark reversion of Pfr (Mumford & Jenner, 1971). Apparently, no net oxidation of the reducing agents occurs during the dark reversion of Pfr. Thus, dithionite enhances the dark reversion rate and counteracts the inhibitory effect of ANS without affecting the faster kinetic component (Figure 8 and Table V). It is likely that the site of dithionite catalysis is at the slower component, k_2',

in Scheme I. It is possible that ANS binds at the Pfr chromophore site (in Pfr′ form), in competition with the chromophore, while dithionite complexes with the chromophore probably via charge-transfer interactions, the latter acting as an electron acceptor.[3] Accompanying the red shift of Q_y band of Pr at 660 nm to 730 nm for Pfr as a result of phototautomerically extended conjugation of the chromophore (Song et al., 1979), the Koopmans' theorem of the electron affinity of chromophores predicts an increase upon Pr → Pfr transformation (Y. Kwak and P. S. Song, unpublished data). Thus, charge-transfer interactions between reducing agents and the chromophore of Pfr without net oxidation of the former may account for the structural diversity of reducing agents which accelerate the dark reversion of Pfr. The accelerating effects of Ca^{2+} and Mg^{2+} (Negbi et al., 1975) can also be accommodated in Scheme I, namely that these cations facilitate hydrophobic interactions between the Pfr chromophore and its binding surface on the protein. Reducing agents are unable to complex with Pr since the chromophore here is not as exposed as in Pfr (Song, 1980a; Hahn et al., 1980).

Conclusions

ANS binds both the Pr and Pfr forms of phytochrome, with an additional affinity for the latter. The specific site of ANS binding on the Pfr form appears to be the hydrophobic surface area of the protein which becomes fully, or at least partially, exposed in the Pfr form and where the hydrophobic fluorescence probe ANS competitively binds to produce the enhanced fluorescence emission and the inhibition of the photoreversion and dark reversion. ANS affects only the slower component of biphasic kinetics in Pfr dark reversion, which is accelerated by sodium dithionite. We propose a consecutive kinetic scheme in which a Pfr intermediate is selectively quenched by ANS, depriving the Pfr chromophore of its hydrophobic binding surface on the protein, and this is counteracted by dithionite, which complexes with the chromophore via charge-transfer interactions, forcing expulsion of the occupied ANS from the chromophore binding site.

Acknowledgments

The expert assistance of Dr. In-Soo Kim and H. Sarkar is greatly appreciated.

References

Brand, L., & Gohlke, J. R. (1972) *Annu. Rev. Biochem. 41*, 843–868.

Briggs, W. R., & Rice, H. V. (1972) *Annu. Rev. Plant Physiol. 23*, 293–334.

Butler, W. L., Siegelman, H. W., & Miller, C. O. (1964) *Biochemistry 6*, 851–857.

Correll, D. L., Edwards, J. L., & Shropshire, W., Jr. (1968) *Photochem. Photobiol. 8*, 465–475.

Furuya, M. (1976) in *Light and Plant Development* (Smith, H., Ed.) pp 143–155, Butterworth, London.

Hahn, T. R., Kang, S. S., & Song, P. S. (1980) *Biochem. Biophys. Res. Commun. 97*, 1317–1323.

Hendricks, S. B., Butler, W. L., & Siegelman, H. W. (1962) *J. Phys. Chem. 66*, 2550–2555.

Hunt, R. E., & Pratt, L. H. (1979) *Plant Physiol. 64*, 332–336.

Hunt, R. E., & Pratt, L. H. (1981) *Biochemistry 20*, 941–945.

Jung, J., & Song, P. S. (1979) *Photochem. Photobiol. 29*, 419–421.

Jung, J., Song, P. S., Paxton, R. J., Edelstein, M. S., Swanson, R., & Hazen, E. E., Jr. (1980) *Biochemistry 19*, 24–32.

Kendrick, R. E., & Spruit, C. J. P. (1977) *Photochem. Photobiol. 26*, 201–214.

Killilea, S. D., O'Carra, P., & Murphy, R. F. (1980) *Biochem. J. 187*, 311–320.

Kim, I. S., Hahn, T. R., & Song, P. S. (1981) *Photochem. Photobiol.* (in press).

Klein, G., & Rüdiger, W. (1978) *Liebigs Ann. Chem. 2*, 267–279.

Lagarias, J. C., & Rapoport, H. (1980) *J. Am. Chem. Soc. 102*, 4821–4828.

Lakowicz, J. R., Cherek, H., & Bevan, D. R. (1980) *J. Biol. Chem. 255*, 4402–4403.

Manabe, K., & Furuya, M. (1971) *Plant Cell Physiol. 12*, 95–101.

Mumford, F. E., & Jenner, E. L. (1966) *Biochemistry 5*, 3657–3662.

Mumford, F. E., & Jenner, E. L. (1971) *Biochemistry 10*, 98–101.

Negbi, M., Hopkins, D. W., & Briggs, W. R. (1975) *Plant Physiol. 56*, 157–159.

Oh, S. (1980) Ph.D. Dissertation, Texas Tech University, Lubbock, TX.

Penzer, G. R. (1972) *Eur. J. Biochem. 25*, 218–228.

Pike, C. S., & Briggs, W. R. (1972) *Plant Physiol. 49*, 514–520.

Pratt, L. H. (1978) *Photochem. Photobiol. 27*, 81–105.

Quail, P., Marmé, D., & Schäfer, E. (1973) *Nature (London), New Biol. 245*, 189–191.

Roux, S., Jr., & Hillman, W. S. (1970) *Arch. Biochem. Biophys. 131*, 423–429.

Rüdiger, W. (1980) *Struct. Bonding 41*, 101–141.

Satter, R. L., & Galston, A. W. (1976) in *Chemistry and Biochemistry of Plant Pigments* (Goodwin, T. W., Ed.) Vol. 1, pp 680–735, Academic Press, New York.

Smith, W. O., & Daniels, S. (1980) *Plant Physiol. (Suppl.) 65*, 2.

Song, P. S. (1978) *Annu. Rep. Prog. Chem., Sect. B: Phys. Methods Tech. 74*, 18–44.

Song, P. S. (1980a) in *Photoreception and Sensory Transduction in Aneural Organisms* (Lenci, F., & Colombetti, G., Eds.) pp 235–240, Plenum Press, New York.

Song, P. S. (1980b) *Proc. Int. Congr. Photobiol. (Strasbourg)*, Abstract, p 100.

Song, P. S., Chae, Q., & Gardner, J. G. (1979) *Biochim. Biophys. Acta 576*, 479–495.

Spencer, R. (1970) Ph.D. Dissertation, University of Illinois, Urbana, IL.

Spencer, R., & Weber, G. (1969) *Ann. N.Y. Acad. Sci. 158*, 361–376.

Taylor, A. O. (1968) *Plant Physiol. 43*, 767–774.

Tobin, E. M., & Briggs, W. R. (1973) *Photochem. Photobiol. 18*, 487–495.

Van Liew, H. D. (1967) *J. Theor. Biol. 16*, 43–53.

[3] Dithionite had no effect on Pr → Pfr and Pfr → Pr phototransformations even after three photocyclings of phytochrome in the presence of 2 mM dithionite. This suggests that the Pr → Pfr transformation does not involve a photooxidation of chromophore with disulfide in the Pr protein.